Published in final edited form as:
Aging Cell. 2008 June ; 7(3): 405–417. doi:10.1111/j.1474-9726.2008.00384.x.

Manganese superoxide dismutase activity regulates transitions between quiescent and proliferative growth

Ehab H. Sarsour, **Sujatha Venkataraman**, **Amanda L. Kalen**, **Larry W. Oberley**, and **Prabhat C. Goswami**[1]
Free Radical and Radiation Biology Program, Department of Radiation Oncology, University of Iowa, Iowa City, USA

SUMMARY

In recent years, the intracellular reactive oxygen species (ROS) levels gained increasing attention as a critical regulator of cellular proliferation. We investigated the hypothesis that manganese superoxide dismutase (MnSOD) activity regulates proliferative and quiescent growth by modulating cellular ROS levels. Decreasing MnSOD activity favored proliferation in mouse embryonic fibroblasts (MEFs), while increasing MnSOD activity facilitated proliferating cells' transitions into quiescence. MnSOD (+/−) and (−/−) MEFs demonstrated increased superoxide steady-state levels; these fibroblasts failed to exit from the proliferative cycle, and showed increasing cyclin D1 and cyclin B1 protein levels. MnSOD (+/−) MEFs exhibited an increase in the percentage of G_2 cells compared to MnSOD (+/+) MEFs. Overexpression of MnSOD in MnSOD (+/−) MEFs suppressed superoxide levels and G_2 accumulation, decreased cyclin B1 protein levels, and facilitated cells' transit into quiescence. While ROS are known to regulate differentiation and cell death pathways both of which are irreversible processes, our results show MnSOD activity and therefore, mitochondria-derived ROS levels regulate cellular proliferation and quiescence, which are reversible processes essential to prevent aberrant proliferation and subsequent exhaustion of normal cell proliferative capacity. These results support the hypothesis that MnSOD activity regulates a mitochondrial "ROS-Switch" favoring a superoxide-signaling regulating proliferation and a hydrogen peroxide-signaling supporting quiescence.

Keywords

MnSOD; Cyclin D1; Cyclin B1; ROS; Cell Cycle; Antioxidant Enzymes; superoxide; hydrogen peroxide

INTRODUCTION

Cellular redox environment is influenced by the production of reactive oxygen species (ROS) and their removal by antioxidants. ROS (superoxide, hydrogen peroxide, hydroxyl radical,

Corresponding author: Prabhat C. Goswami, Ph.D., Free Radical & Radiation Biology Program, Department of Radiation Oncology, The University of Iowa, B180 Medical Laboratories, Iowa City, Iowa-52242, *phone:* (319) 384-4666, *fax:* (319) 335-8039, prabhat-goswami@uiowa.edu.

We thank Dr. Garry R. Buettner and the EPR core facility for assistance with EPR spectroscopy, Mr. Burl E. Hess and the flow cytometry core facility for assisting with flow cytometry, and Mr. Zhen Gao for assisting with the real time RT-PCR assay. Funding from NIH CA 111365 and McCord Research Foundation supported this work.

Abbreviations used: AdBgl II: adenovirus containing an empty vector; AdMnSOD: adenovirus containing mouse MnSOD cDNA; AdmMnSOD: adenovirus containing human mutant MnSOD cDNA; BrdU: bromodeoxyuridine; DCFH: 5-(and 6)-chloromethyl-2`, 7`-dichlorodihydro fluorescein diacetate; DHE: dihydroethidium; DMPO: 5, 5-dimethyl-1-pyrroline N-oxide; EPR: electron paramagnetic resonance; RNS: reactive nitrogen species; ROS: reactive oxygen species

singlet molecular oxygen, and organic hydroperoxides) are primarily produced intracellularly by two metabolic sources: the mitochondrial electron transport chain and enzymatic reactions. ROS levels are tightly regulated by antioxidant enzymes and small molecular weight antioxidants (McCord & Fridovich 1969; Oberley 1982; Fernandes & Holmgren 2004). MnSOD is a nuclear encoded and mitochondrial matrix-localized antioxidant enzyme that catalyzes the conversion of superoxide to hydrogen peroxide, which is further converted to water by glutathione peroxidase and catalase. Traditionally, ROS were thought to be toxic by-products of living in an aerobic environment, causing damage to cellular macromolecules. However, in recent years, it is increasingly evident that ROS-levels regulate multiple cellular processes, including proliferation (Burdon & Gill 1993; Sundaresan *et al.* 1995; Bae *et al.* 1997; Irani *et al.* 1997).

Previous studies reported ROS-signalling, regulates cellular proliferation in response to mitogenic stimuli including platelet derived growth factor, epidermal growth factor, cytokine, antigen receptors, and oncogenic Ras (Sundaresan *et al.* 1995; Bae *et al.* 1997; Irani *et al.* 1997). Results from these previous studies suggested membrane-bound NADPH-oxidase as the source of ROS-signalling. We have shown previously that the cellular redox environment could regulate cell cycle phase transitions (Goswami *et al.* 2000; Menon *et al.* 2003; Sarsour *et al.* 2005; Menon & Goswami 2007). Mitochondria being the major source of cellular ROS it is important to determine if MnSOD activity and mitochondria-generated ROS regulate normal cell proliferation.

Normal cell proliferation has two distinctive stages: the proliferative cycle and quiescent growth. The proliferative cycle includes entry into, and progression through the cell cycle. It also includes transitioning into the quiescent growth, which is essential to prevent aberrant proliferation as well as protecting cellular lifespan. Transition from quiescence (G_0) to proliferative growth (G_1 to S to G_2 and M) involves the sequential activation of cyclin dependent kinase activities (Sherr 1993; Grana & Reddy 1995). Progression from G_0/G_1 to S is largely regulated by the D-type cyclins in association with the cyclin dependent kinases, CDK4/6. Cyclin D1/CDK4–6 kinase complex partially phosphorylates the retinoblastoma (Rb) protein, causing the release of the E2F family of proteins, which transcriptionally activates expression of multiple S-phase specific genes required for DNA replication (Nevins 1992). Cyclin B1/CDK1 kinase complex, along with Cdc25C phosphatase, regulates progression from G_2 to M phase. Because cyclins are the positive regulators of cellular proliferation, cyclin D1 and cyclin B1 protein levels are often used as indicators of cells entering into and exiting from the proliferative cycle.

We investigated the hypothesis that MnSOD activity regulates transitions between proliferative and quiescent growth by modulating cellular ROS (superoxide and hydrogen peroxide) levels. Our results show a decrease in MnSOD activity, and therefore an increase in superoxide steady state levels, promotes proliferation. In contrast, an increase in MnSOD activity and the resultant decrease in superoxide levels support quiescence. Decreasing MnSOD activity was associated with an increase in cyclin D1 and cyclin B1 protein levels supporting proliferative growth, while increasing MnSOD activity decreased cyclin B1 and facilitated fibroblasts' transition into quiescent growth.

RESULTS

MnSOD activity regulates transitions between quiescent and proliferative growth

Initially, we determined if changes in MnSOD activity affects cellular superoxide steady state levels and activities of other antioxidant enzymes. Exponentially growing asynchronous cultures of mouse embryonic fibroblasts (MEFs) were harvested and total cellular protein extracts were used for measurement of antioxidant enzyme activity. MnSOD activity was

higher in wild type (+/+) compared to the heterozygous (+/−) cells and absent in homozygous knock-out (−/−) MEFs (Fig. 1A). Changes in MnSOD activity did not significantly alter CuZnSOD and catalase activities. Cells from replicate dishes were collected for EPR spectroscopy measurements of superoxide steady state levels (Fig. 1A, bottom panel). The steady state levels of superoxide was low in MnSOD (+/+) MEFs and increased ~5-fold in MnSOD (+/−) MEFs. MnSOD (−/−) MEFs showed ~9-fold higher levels of superoxide compared to MnSOD (+/+) MEFs.

To determine if MnSOD activity regulates cellular proliferation, cell growth was measured in MnSOD (+/+), MnSOD (+/−) and MnSOD (−/−) MEFs. Results from the cell growth assay showed all three cell types had an initial lag-period followed by exponential growth (Fig. 1B). MnSOD (+/+) fibroblasts reached confluence (quiescence; <5% S-phase) between 6 and 9d post-plating. MnSOD (+/−) fibroblasts continued to grow and failed to exit from the proliferative cycle. MnSOD (−/−) had a much longer lag-period and cell proliferation was significantly suppressed. Cell population doubling time for the three cell types were as follows: MnSOD (+/+), 41h; MnSOD (+/−), 47h; MnSOD (−/−), 110h.

MnSOD activity was lower in wild type exponential cultures and increased as cells transitioned into quiescence (Fig. 1B inset). The growth state-dependent changes in MnSOD activity were independent of MnSOD protein levels and mRNA, which did not show any difference in quiescent growth (9d post-plating) compared to exponential growth (4d post-plating, Fig. 1B inset and data not shown). MnSOD activity remained low in MnSOD (+/−) MEFs at 6 and 9d post-plating, which is consistent with these cells' inability to exit from the proliferative cycle.

To determine if MnSOD activity regulates progression through the proliferation cycle, fibroblasts from replicate dishes were trypsinized and fixed in ethanol. Ethanol-fixed cells were analyzed for DNA content by flow cytometry. Representative DNA histograms are shown (Fig. 1C, upper panels) and quantitation of results is presented (Fig. 1C, lower panels). The percentage of S-phase cells was higher (23%) at 2d post-plating in MnSOD (+/+) fibroblasts, gradually decreasing to less than 4% at 12d post-plating as cells transitioned into quiescence. These results suggest that MnSOD (+/+) MEFs retained the capacity to successfully transit into quiescence from the proliferative growth state.

The extended lag-period in MnSOD (−/−) fibroblasts' growth (Fig. 1B) was associated with a large increase in the percentage of cells with sub-G_1 DNA content (Fig. 1C); indicating an absence of MnSOD activity resulted in extensive cell loss. However, it appears MnSOD (−/−) fibroblasts must have adapted to proliferation because the percentage of cells with sub-G_1 DNA content decreased at 12d post-plating, coinciding with an increase in the percentage of S-phase (14–16%) as well as an increase in cell number.

The percentage of S-phase in MnSOD (+/−) fibroblasts was ~15% at day 2 and remained relatively constant during the 12d of culture, indicating a decrease in MnSOD activity inhibited MEFs exit from the proliferative cycle (Fig. 1C). The percentages of G_2+M-phases in MnSOD (+/+) and MnSOD (−/−) MEFs were comparable. However, MnSOD (+/−) fibroblasts exhibited a significantly higher percentage (>40%) of cells in G_2+M (Fig. 1C).

A BrdU-pulse chase assay was used to determine if the increase in percent G_2 in MnSOD (+/−) MEFs could be due to a delay in G_2-transit (Fig. 2). Exponentially growing asynchronous cultures were pulse-labelled with BrdU and continued in culture in BrdU-free media. MEFs were harvested at various times post-BrdU-labelling, and ethanol-fixed cells were assayed for BrdU positive and negative population by flow cytometry. Three distinct cell populations, BrdU-positive S-phase and BrdU-negative G_1 and G_2 were detected at the end of 30 min BrdU-labelling for both cell types (Fig. 2A). Representative histograms demonstrating cell cycle progression at 2, 4, and 8h post-BrdU labelling are presented in figure 2A. Results showed

cells in G_2 progressed normally to M phase with a median transit duration of approximately 3h in MnSOD (+/+) fibroblasts (Fig. 2B, left panel). However, the median G_2-transit time was higher (>8h) in MnSOD (+/−) fibroblasts. Likewise, the fraction of BrdU-positive cells completing cell division (cells in box marked $G_1{}^+$) was higher in MnSOD (+/+) *vs.* MnSOD (+/−) fibroblasts (Fig. 2B, right panel) suggesting the duration of transit through G_2 and M phases was longer in MnSOD (+/−) compared to MnSOD (+/+) MEFs.

Next we determined if the delay in G_2+M transit could be due to MnSOD (+/−) MEFs' inability to maintain an appropriate superoxide threshold level. MnSOD (+/−) fibroblasts were treated with a superoxide scavenging agent Tiron and cells were harvested for EPR and flow cytometry measurements. Tiron decreased the superoxide steady state levels by approximately 50%; these cells also exhibited a decrease in the percentage of cells in G_2-phase (25% in control *vs.* 10% in Tiron-treated cells; Fig. 2D, left panel). In a separate experiment, asynchronously growing exponential cultures of MnSOD (+/+) fibroblasts were infected with adenovirus carrying a dominant negative mutant form of MnSOD, and cells were harvested for measurements of superoxide steady state levels and percent G_2+M. Overexpression of the mutant MnSOD showed a significant decrease in MnSOD activity (Fig. 2E, inset). The decrease in MnSOD activity was associated with a 4-fold increase in the percentage of cells in G_2+M phase (Fig. 2E). These results were comparable with results obtained from the MnSOD (+/−) MEFs suggesting that the cells' failure to maintain an appropriate superoxide threshold level could affect G_2+M transit and subsequent transition into quiescent growth in daughter generations.

To determine if MnSOD activity regulates quiescent fibroblasts' entry into the proliferative cycle, 10 and 30d quiescent MEFs were re-plated at a lower cell density and cell growth measured for 6d (Fig. 3). Cell cycle phase distributions prior to re-plating were assayed by flow cytometry analysis of DNA content. While the percentage of G_1 cells were higher in 30d compared to 10d MnSOD (+/+) MEFs, the percentage of G_1 cells did not differ in 10 and 30d cultures of MnSOD (+/−) and (−/−) MEFs (Fig. 3A). The percentage of S-phase cells was higher in MnSOD (+/−) and (−/−) MEFs compared to wild type cells suggesting that these cells might not have exited from the proliferative cycle. MEFs sub-cultured from 10d confluent cultures showed comparable growth characteristics among the three cell types (Fig. 3B, left panel). Interestingly, while cell growth was comparable in fibroblasts sub-cultured from 30d MnSOD (+/−) and (−/−) MEFs, it was significantly inhibited in MnSOD (+/+) MEFs (Fig. 3B, right panel).

MnSOD activity regulated transition from quiescent to the proliferative cycle was further evident from the results presented in figure 3C. Quiescent cultures of MnSOD (+/+) MEFs were infected with adenovirus carrying a dominant negative mutant form of MnSOD (AdmMnSOD) cDNA and assayed for MnSOD activity and superoxide levels. Overexpression of the dominant negative mutant MnSOD significantly increased superoxide levels (Fig. 3C). Control and adenovirus infected cells were re-plated at lower cell density and harvested at 48h post-replating for flow cytometry analysis of cell cycle phase distributions. The percentage of G_1-cells decreased in control and AdBgl II infected fibroblasts suggesting that these cells entered into S-phase. The percentage of G_1 cells was higher in AdmMnSOD overexpressing MEFs indicating that appropriate amount of MnSOD activity during quiescence is required to maintain MEFs capacity to re-enter the proliferative cycle. Similar results were obtained from quiescent normal human skin fibroblasts (NHFs) that were infected with AdmMnSOD (Supplemental Results, Fig. S1). Quiescent NHFs were infected with adenoviruses carrying wild type and mutant form of human MnSOD cDNAs. Control and adenovirus-infected cells were replated at a lower cell density and cell numbers counted at 2, 4, and 6d post-plating. Cell growth was significantly suppressed in AdmMnSOD infected cells compared to control and AdMnSOD infected cells (Supplemental Results, Fig. S1).

MnSOD activity-regulated transitions between quiescence and proliferative growth are associated with changes in cyclin D1 and cyclin B1 protein levels

To determine whether MnSOD activity could influence cell cycle regulatory proteins, immunoblotting assays were performed using total cellular protein extracts isolated from MnSOD (+/+) and MnSOD (+/−) fibroblasts harvested at indicated times. These measurements were not made in MnSOD (−/−) MEFs because of extensive cell death and subsequent aberrant proliferation indicating that these cells might have undergone transformation (see below). Both cyclin D1 and cyclin B1 protein levels decreased in MnSOD (+/+) fibroblasts as cells exited from the proliferative cycle. Cyclin D1 protein levels decreased to 17%, and cyclin B1 protein levels decreased to 14% at 9d post-plating (Fig. 4A). The decrease in cyclin D1 and B1 protein levels corresponded to a decrease in S-phase from 25 to <5%. However, cyclin D1 and B1 protein levels showed minimal changes in MnSOD (+/−) fibroblasts during 4–9 d post-plating (Fig. 4A), correlating with cells' inability to exit from the proliferative cycle.

In a separate series of experiments, it was determined whether MnSOD overexpression could facilitate MnSOD (+/−) fibroblasts' exit from the proliferative cycle. MnSOD (+/−) MEFs were infected with adenovirus carrying mouse wild type MnSOD cDNA (AdMnSOD) and then harvested for measurements of MnSOD activity, superoxide steady state levels, and cyclin B1 protein levels. MnSOD overexpression exhibited a dose-dependent increase in MnSOD activity (Fig. 4B). This increase corresponded to a decrease in superoxide steady state levels (Supplemental Results, Fig. 3). Furthermore, MnSOD (+/−) fibroblasts infected with 50 and 100 MOI AdMnSOD significantly decreased cyclin B1 protein levels (Fig. 4B). At 3d post-infection, cell numbers were similar in MnSOD (+/−) control, AdBgl II, and AdMnSOD infected cells (Fig. 4C). The cell numbers in MnSOD (+/−) fibroblasts control, AdBgl II, and 30 MOI AdMnSOD infected cells continued to increase at 6d post-infection. However, MnSOD (+/−) fibroblasts infected with 100 MOI AdMnSOD showed no change in cell numbers at 6 *vs.* 3d post-infection (Fig. 4C). These results suggest MnSOD overexpression facilitated MnSOD (+/−) MEFs' transition from the proliferative to quiescent growth.

Decrease in MnSOD activity was associated with aberrant proliferation

The hypothesis that MnSOD activity regulates transitions between proliferative and quiescent growth was further evident in long-term cultures. MEFs were maintained in cultures with regular change in growth medium and cell numbers were measured at 6 and 30d post-plating (Fig. 4D). Cell numbers in MnSOD (+/+) fibroblasts were comparable at 6 and 30d post-plating, suggesting these cells exited from the proliferative cycle and maintained quiescent growth. However, cell numbers in MnSOD (+/−) and MnSOD (−/−) fibroblasts continued to increase, suggesting these cells failed to exit from the proliferative cycle (Fig. 4D, left panel). The aberrant proliferation in MnSOD (+/−) and (−/−) MEFs were also evident in long-term culture dishes stained with Coomassie dye (Fig. 4D, right panel). MnSOD (+/+) fibroblasts exhibited contact inhibited monolayer cultures characteristic of normal cell growth. In contrast, cell densities were significantly higher in MnSOD (+/−) fibroblasts and isolated foci with intense cell growth were observed in MnSOD (−/−) fibroblasts.

MnSOD activity regulates an ROS-switch during transitions between proliferative and quiescent growth

MnSOD activity converts superoxide produced in the mitochondria to hydrogen peroxide, thereby regulating cellular ROS steady state levels. To determine if changes in ROS levels are associated with transitions between proliferative and quiescent growth, DHE (indicative of superoxide) and DCFH (indicative of hydrogen peroxide) fluorescence were measured by flow cytometry. The specificity of DHE and DCFH assays for measurements of superoxide and hydrogen peroxide levels is shown in results presented in figure 3C and supplemental figure S2. Results (Fig. 5A) showed steady state levels of superoxide were higher in MnSOD (+/+)

exponential cultures (2d post-plating, 20–25% S-phase) compared to quiescent growth (20d post-plating, <5% S-phase). Hydrogen peroxide levels were lower in exponential cultures (2d post-plating) compared to quiescent cultures (20d post-plating, Fig. 5B). The steady state levels of superoxide in MnSOD (+/−) and MnSOD (−/−) fibroblasts were higher both in 2 and 20d cultures. The increase in superoxide and decrease in hydrogen peroxide levels in MnSOD (+/−) and (−/−) fibroblasts in 20d cultures were associated with cells' inability to exit from the proliferative cycle. Consistent with these results, the percentage of S phase cells remained higher in MnSOD (+/−) and (−/−) MEFs (15 and 25%, respectively). Interestingly, a direct correlation was observed between superoxide levels and percent S phase (R^2=0.95, Fig. 5C).

The concept of mitochondria-derived ROS regulating quiescent and proliferative growth was further supported by results presented in figure 6. Exponential and quiescent cultures of MnSOD (+/+) MEFs were assayed for extracellular hydrogen peroxide levels using the HRP-pHPA method (Fig. 6A). Hydrogen peroxide levels were low in exponential cultures and increased ~4-fold in quiescent cultures. The specificity of the assay for hydrogen peroxide measurements was determined using catalase in the reaction buffer. Catalase treatment neutralized hydrogen peroxide both in exponential and quiescent cultures (Fig. 6A, upper panel). The increase in hydrogen peroxide levels was associated with a decrease in the percentage of S-phase cells (Fig. 6A, bottom panel). In a separate set of experiments, exponential and quiescent cultures of MnSOD (+/+) MEFs were incubated with MitoSox and MitoTracker dyes and fluorescence measured by flow cytometry. MitoTracker fluorescence was comparable in exponential and quiescent cultures. However, exponential cultures showed significantly higher (~4–5 folds) MitoSox fluorescence compared to quiescent cultures (Fig. 6B). These results were consistent with results presented in figure 5 supporting the hypothesis that mitochondria-generated ROS could regulate transitions between quiescent and proliferative growth.

DISCUSSION

The concept of cellular redox environment regulating proliferation can be traced back to 1931 when Rapkine first demonstrated the presence of soluble thiols that fluctuated cyclically during cell division in sea urchin eggs (Rapkine 1931). Later in 1960, Kawamura *et al* showed increased protein thiol-staining as the mitotic spindle was assembling in sea urchin eggs (Kawamura 1960). Subsequently, Mauro and Tolmach reported that the protein-bound and non-protein sulfhydryl (-SH) and disulfide (-SS-) groups oscillate during the mammalian cell cycle (Mauro *et al.* 1969). Consistent with these earlier observations, we reported previously that the fluorescence of a pro-oxidant sensitive dye increased 2–3 fold in G_2 compared to G_1, a pro-oxidant event is necessary prior to S-entry, and pharmacological manipulations of cellular redox environment resulted in G_1-delay (Goswami *et al.* 2000; Menon *et al.* 2003; Menon *et al.* 2005; Sarsour *et al.* 2005). While these previous reports support the hypothesis of cellular ROS regulating proliferation, a direct relationship between antioxidant enzyme, ROS, and cell proliferation is currently lacking.

The present study was designed to determine if MnSOD activity and therefore, mitochondria derived ROS regulate transitions between quiescent and proliferative growth. Mouse embryonic fibroblasts with MnSOD wild type (+/+), (+/−) and (−/−) genotypes were used to demonstrate that MnSOD activity regulates cellular ROS levels favouring a superoxide-signalling regulating proliferation and hydrogen peroxide-signalling supporting quiescent growth. For many years, ROS were only thought to be toxic unwanted by-products of living in an aerobic environment. It was suggested ROS cause random damage to cellular macromolecules and this cumulative-damage of critical cellular macromolecules is believed to be the cause of slow degeneration of biological systems during the aging process. This idea was originally proposed in the Free Radical Theory of Aging and Oxygen Toxicity (Harman

1956). However, numerous recent reports, including our own research, suggest ROS are essential physiological requirements for maintaining cellular redox-homeostasis, and that lower levels of ROS, in fact, act as secondary messengers regulating multiple cellular processes including proliferation.

Our results show mouse embryonic fibroblasts with different MnSOD-genotypes exhibited discrete differences in cellular proliferation. MnSOD (+/+) fibroblasts demonstrated an initial lag-period followed by exponential and quiescent growth, characteristics of normal cellular proliferation (Fig. 1). An additional characteristic of normal cell proliferation relates to the gradual loss in proliferation capacity of quiescent cells. We have defined previously this property of normal cell as the telomerase-independent non-replicative senescence (Sarsour *et al.* 2005). MnSOD (+/+) fibroblasts sub-cultured from 10 and 30d quiescent growth showed significant differences in their proliferative capacity. The percentage of S-phase decreased to approximately 5% at 48h of re-plating of 30d quiescent cultures, which correlated with an inhibition in cell growth.

Although MnSOD (+/−) and (−/−) fibroblasts exhibited an initial lag-period followed by exponential growth, these cells were unable to exit from the proliferation cycle and failed to establish quiescent growth (Fig. 1). Likewise, both cell types maintained their proliferative capacities upon sub-culturing from 10 and 30d cultures (Fig. 3). Additional differences were also observed in exponential cultures of MnSOD (+/−) and MnSOD (−/−) fibroblasts compared to wild type cells. MnSOD (+/−) fibroblasts showed a significant increase in percentage of G_2 cells. Results from the BrdU-pulse-chase assay demonstrated the increase in the percentage of G_2 cells in MnSOD (+/−) fibroblasts was primarily due to a delayed transit through G_2, indicating an appropriate amount of MnSOD activity is required for progression from G_2 to M and subsequent exit from the proliferative cycle in daughter generations (Fig. 2). MnSOD (−/−) fibroblasts maintained a higher percentage of cells with sub-G_1 DNA content until 9d post-plating (Fig. 1). This increase in the percentage of cells with sub-G_1 DNA content suggested the lack of MnSOD activity is detrimental to cells. However, it appears that MnSOD (−/−) fibroblasts overcame this initial wave of cell loss during 9-12d post-plating and adapted to proliferation, which is indicated by a corresponding increase in S-phase percentage. These results clearly suggest MnSOD activity is required for proper transitions between quiescent and proliferative growth.

A key concept emerged from our results, which indicates MnSOD activity regulates an “ROS-switch” favouring a superoxide-signal regulating proliferation and a hydrogen peroxide-signal supporting quiescent growth. MnSOD is a nuclear encoded mitochondrial localized antioxidant enzyme known to convert mitochondrial-generated superoxide to hydrogen peroxide. Therefore, changes in MnSOD activity are anticipated to influence cellular ROS steady state levels. Consistent with this hypothesis our results show increased superoxide steady state levels in exponential cultures of all three MnSOD genotype fibroblasts (Fig. 5). In fact, a direct correlation was observed between superoxide steady state levels and percent S phase (R^2=0.95, Fig. 5). Consistent with this correlation, superoxide steady state levels were low as MnSOD (+/+) fibroblasts exited from the proliferative cycle, which was accompanied with an increase in hydrogen peroxide levels in quiescent growth (Fig. 5). This growth-state related transition from superoxide to hydrogen peroxide was absent in MnSOD (+/−) and (−/−) fibroblasts, and accordingly these cells failed to exit from the proliferative cycle. The failure to exit from the proliferation cycle in MnSOD (+/−) fibroblasts was probably due to a slower exit from G_2 because scavenging of superoxide with Tiron (or overexpressing MnSOD) decreased G_2-delay and these cells subsequently exited from the proliferation cycle (Fig. 2C&D). The concept of an “ROS-switch” regulating periodic events during cellular proliferation is further supported by a recent report (Tu *et al.* 2005). These authors demonstrated budding yeast exhibits a metabolic redox-cycle consisting of a reductive non-respiratory phase and an oxidative

respiratory phase. This metabolic redox cycle coordinates with periods of gene expression regulating essential cellular and metabolic events. The initiation of cell cycle occurs very late during the oxidative phase and the reductive phase triggers expression of many of the genes required for DNA replication. Our results show an inverse correlation between the percentage of S-phase and extracellular hydrogen peroxide levels (Fig. 6A). Extracellular hydrogen peroxide levels were lower in exponential compared to quiescent MnSOD (+/+) MEFs. Interestingly, MitoSox-fluorescence was higher in exponential compared to quiescent MnSOD (+/+) MEFs (Fig. 6B). These results are consistent with results presented in figure 5 supporting the hypothesis that MnSOD activity and mitochondrially-generated ROS-levels could link cellular metabolism to proliferative and quiescent growth (Fig. 7).

Recent evidence suggests that ROS could reversibly modify the redox-state of specific cysteine in phosphatases (protein tyrosine phosphatases and dual specificity phosphatases) inactivating their activities, which could favour Ser/Thr phosphorylation-dependent signal pathways initiating proliferation (Finkel 2003; Rhee *et al.* 2003; Tonks 2005). While the source of ROS is not completely understood, it is suggested that ROS generated from membrane-localized NADPH-oxidase could initiate the signalling cascades. Our results indicate that a cross-talk between MnSOD-activity (possibly *via* mitochondria-derived ROS-levels pathways) and cell cycle regulatory proteins could significantly influence the transitions between quiescent and proliferative growth. Consistent with this hypothesis MnSOD activity and ROS-levels were found to be associated with changes in cyclin D1 and cyclin B1 protein levels. Cyclin D1 is believed to be the first cell cycle regulatory protein that responds to mitogenic stimuli facilitating cells' entry into S-phase. Cyclin B1 is known to regulate progression from G_2 to M. Both protein levels were higher in asynchronously growing exponential cultures of MnSOD (+/+) fibroblasts, and decreased as cells exited from the proliferative cycle (Fig. 4). Cyclin D1 and cyclin B1 protein levels remained high in MnSOD (+/−) fibroblasts, consistent with their failure to exit from the proliferative cycle (Fig. 1&Fig. 7). However, overexpression of MnSOD in MnSOD (+/−) fibroblasts decreased cyclin B1 protein levels. These cells managed to exit from the proliferative cycle, indicated by a decrease in superoxide steady state levels and minimal change in cell number between 3 and 6d post-infection (Fig. 4). Although the exact mechanisms of cellular redox environment regulating cell cycle proteins are not completely understood, we have recently shown an inverse correlation between MnSOD activity and cyclin D1 protein levels in NIH3T3 mouse fibroblasts that were treated with the thiol antioxidant, N-acetyl-L-cysteine (NAC). NAC treatment increased MnSOD protein levels and activity while decreasing cyclin D1 protein levels. NAC-induced decrease in cyclin D1 was abrogated in NIH3T3 fibroblasts overexpressing a mutant form of cyclin D1 (T286A). Since phosphorylation at T286 targets cyclin D1 for degradation we speculated NAC-induced increase in MnSOD activity could modulate redox-sensitive pathways affecting T286-phosphorylation and subsequent degradation of cyclin D1 (Menon *et al.*, 2007). These results support the hypothesis that the cellular redox environment coordinates cell cycle regulatory protein expression during transitions between quiescent and proliferative growth.

While ROS are known to regulate differentiation and cell death pathways both of which are irreversible processes, our results show mitochondria-derived ROS regulates cellular proliferation and quiescence, which are reversible processes essential for cell and tissue renewals. Furthermore, it is also well known that many cytokines produce ROS/RNS during the inflammation process. Cells respond to these fluxes in ROS/RNS by enhancing antioxidant enzymes gene expression including the expression of MnSOD. Inflammation-induced increase in MnSOD activity while serves as ROS-scavengers, our results suggest MnSOD activity could also influence cell growth by regulating transitions between quiescent and proliferative growth states. At present, it is unclear how the same ROS could regulate such diverse biological processes that include proliferation, quiescence, differentiation, inflammation, and cell death. It is hypothesized that location of ROS-generation and "ROS threshold levels" are two

significant determinants of these diverse cellular processes. Our results indicate mitochondrially-generated ROS levels could be a major mediator linking cellular metabolism to the proliferative and quiescent growth states (Fig. 7).

Our results also suggest that MnSOD activity and mitochondria-derived ROS levels are critical for the maintenance of quiescence to prevent aberrant proliferation and subsequent exhaustion of normal cell proliferative capacity. Our results resemble recent reports of ROS regulating the proliferative capacity of haematopoietic stem cells (Tothova *et al.* 2007). FoxO transcription factor-deficient haematopoietic stem cells (HSCs) showed reduced ability to repopulate. Because FoxO is known to regulate antioxidant enzyme (MnSOD and catalase) gene transcription (Kops *et al.* 2002a; Kops *et al.* 2002b), it was suggested that ROS could mediate the proliferative capacity of quiescent HSCs. Surprisingly, while treatment of FoxO-deficient HSCs with ROS-scavenger, N-acetyl-L-cystine (NAC), restored quiescent HSCs' repopulating ability these treatments also resulted in increased antioxidant enzyme levels. These previously published results suggest ROS could activate additional pathways independent of FoxO to regulate antioxidant enzyme gene expression. We reported previously NAC treated MEFs increased MnSOD protein levels and activity independent of its mRNA levels (Menon *et al.* 2007). Our results from the present study showed significant increase in MnSOD activity (Fig. 1) during transition from the proliferative to quiescent growth, while there were no changes in MnSOD mRNA (data not shown) and protein levels (Fig. 1B). These results suggest post-translational rather than transcriptional mechanisms could regulate MnSOD activity during transitions between quiescent and proliferative growth.

In summary, our results support the hypothesis that MnSOD activity regulates an "ROS-switch" favouring a superoxide-signal regulating the proliferative cycle and a hydrogen peroxide-signal supporting quiescent growth. Higher levels of MnSOD activity were associated with quiescent growth while lower levels support proliferative growth. MnSOD-activity regulated transitions between quiescent and proliferative growth were associated with changes in cyclin D1 and cyclin B1 protein levels. A loss in the redox-control of this regulation could have myriad of cellular effects including aberrant proliferation, defects in cell-renewal, cancer and cellular aging (Fig. 7).

EXPERIMENTAL PROCEDURES

Cell culture

MnSOD wild type (MnSOD +/+), heterozygous (MnSOD +/−), and homozygous knock-out (MnSOD −/−) mouse embryonic fibroblasts (MEFs) primary cultures were generously provided by Dr. T. T. Huang (Stanford University). Normal human skin fibroblast (AG01522C) was purchased from Coriell. Fibroblasts were cultured in Dulbecco's modified Eagle's medium with 10% fetal bovine serum and antibiotics. Monolayer cultures were grown at 37°C in a humidified incubator with 5% CO_2 and 4% oxygen. All experiments were performed within passage 6. Cell cultures with S-phase equal or less than 5% were considered as quiescent growth. Cell population doubling time (Td) was calculated from the exponential portion of the growth curve using the following equation: Td=0.693t/ln(Nt/N0) where t is time in days, and Nt and N0 represent cell numbers at time t and initial time, respectively.

Adenoviral infections

Replication deficient adenoviruses containing cytomegalovirus promoter driven cDNAs for mouse wild type (AdMnSOD) and human mutant (AdmMnSOD) MnSOD were obtained from the University of Iowa DNA-vector Core facility. The mutant form of MnSOD was generated by performing site-directed mutagenesis of histidine-26 to leucine. This substitution in amino acid resulted in a dominant negative function of the protein, which when overexpressed

suppressed the activity of MnSOD (Zhang *et al.* 2006). Adenovirus infections were carried out using exponential and quiescent cultures following our previously published protocol (Sarsour *et al.* 2005). Monolayer cultures were infected with adenoviruses for 24 h in serum free media followed by addition of regular media containing 10% FBS. A non-modified vector (AdBgl II) was used as control for adenoviral infections. Transduction efficiency was measured by flow cytometry assay of AdGFP infected cultures. Transgene expression was verified by immunoblotting and antioxidant enzyme activities measured by native-gel electrophoresis.

Immunoblotting and MnSOD native gel-activity assays

Equal amounts of total cellular proteins were separated by SDS-PAGE and electro-transferred by semi-dry blotting onto a nitrocellulose membrane. Membranes were incubated with antibodies to MnSOD, cyclin D1 (PharMingen BD), and cyclin B1 (Santa Cruz Biotechnology). Immunoreactive bands were detected by an enhanced chemiluminescence kit and results were quantitated using AlphaImager 2000 software (Alpha Innotech). Actin protein levels were used for loading corrections. MnSOD activity was assayed by native gel-electrophoresis following our previously published protocol (Sarsour *et al.* 2005). Briefly, equal amounts of total cellular protein extracts were separated by 12.5% native gel-electrophoresis, and SOD activity determined by incubating the gel with nitroblue tetrazolum NBT (2.43 mM) and riboflavin-TEMED (riboflavin 2.8×10^{-5} M and TEMED 28 mM). Achromatic bands were visualized and quantified using a computerized digital imaging system interfaced with AlphaImager 2000 software (Alpha Innotech., San Leandro,CA).

Quantitative RT-PCR assay

Total cellular RNA was isolated and reverse-transcribed using random-hexamer and reverse transcriptase. cDNAs were PCR-amplified (ABI 7000 Real-Time PCR sequence detection system, Applied Biosystems) using SYBR green and the following primer pairs: MnSOD forward: 5′AGGCTCTGGCCAAGGGAGATGT3′; reverse: 5′ CCACAGACACGGCTGTCAGCTT3′ and 18S rRNA, forward 5′ CCTTGGATGTGGTAGCCGTTT3′; reverse 5′AACTTTCGATGGTAGTCGCCG3′; MnSOD mRNA levels in each sample were normalized to 18S rRNA levels, and relative expression ($2^{-\Delta\Delta CT}$) calculated.

Electron paramagnetic resonance (EPR) measurements of superoxide steady state levels

The EPR spin trapping technique with DMPO as the spin trap was used to detect superoxide levels (Kalen *et al.* 2006). Monolayer cultures were washed with PBS and covered with 500 μL of chelated (iminodiacetic acid, sodium form, Sigma Chemicals) PBS containing 100 mM DMPO. Cells were then incubated at 37°C for 15 min, and transferred to a flat cell for EPR measurement. The specificity of the superoxide signal was determined by pre-incubating the monolayer cells with CuZnSOD (1000 units/ml) or Tiron (1 mM). EPR peak heights were calculated, and normalized to cell number.

Propidium iodide (PI) assay for DNA content

Ethanol-fixed cells were treated with RNase A and PI, and analyzed by flow cytometry for DNA content following our previously published protocol (Menon *et al.* 2003; Sarsour *et al.* 2005).

Bromodeoxyuridine (BrdU) pulse-chase assay

Asynchronously growing exponential MEFs were pulse-labelled with 10-micromolar BrdU for 30 min and continued in BrdU-free culture media. Monolayer cultures were harvested by trypsin and fixed in ethanol. Isolated nuclei were incubated with anti-BrdU antibody (Immunocytometry Systems) followed by incubation with FITC-conjugated goat anti-mouse

IgG. Nuclei were treated with RNase A and counterstained with PI. FITC and PI fluorescence were analyzed on a FACScan flow cytometer (BD Biosciences) following our previously published protocols (Menon *et al.* 2003; Sarsour *et al.* 2005). Data from a minimum of 20,000 nuclei were acquired in list mode and processed using Cellquest Pro software.

Measurement of ROS levels

Monolayer cultures were incubated with Hanks buffer salt solution (HBSS) containing 10 μM DHE (Invitrogen) for 45 min or 1 μg/ml DCFH (Invitrogen) for 15 min. Monolayers were trypsinized and re-suspended in HBSS buffer containing 10% FBS. DHE and DCFH fluorescence were measured by flow cytometry. The flow cytometry measurements of DHE-fluorescence were performed using 488 nm excitation laser and FL2 channel- 585/42 nm band pass emission filter. DCFH fluorescence was measured using 488 nm excitation laser and FL1 channel- 530/30 nm band pass emission filter. Mean fluorescence intensity was analyzed using Flowjo software. Auto-fluorescence of unlabeled cells was used for background fluorescence correction.

Mitochondrial Superoxide measurements

Cell cultures in 60 mm dishes were washed 3 times with warm Hanks buffer salt solution (HBSS), and incubated with 3μM MitoSOX® and 0.5 μM MitoTracker Green® (Invitrogen) for 15 min. Monolayer cultures were trypsinized and re-suspended in HBSS buffer containing 10% FBS. Cell suspensions were washed once and filtered using nylon mesh. Flow cytometry measurements of MitoSOX and MitoTracker fluorescence were performed using 488 nm excitation laser and FL2 channel- 585/42 nm band pass emission filter for MitoSOX and FL1 channel- 530/30 nm band pass emission filter for MitoTracker. Mean fluorescence intensity was analyzed using Flowjo software. Auto-fluorescence of unlabeled cells was used for background fluorescence correction.

Measurement of extracellular hydrogen peroxide

Measurement of H_2O_2 released from quiescent and exponential MnSOD (+/+) MEFs was performed following previously published protocol (Panus *et al.* 1993). This method is based on the reaction of H_2O_2 with horseradish peroxidase (HRP) forming compound I, followed by a subsequent reaction where compound I with *p*-hydroxyphenyl acetic acid (pHPA) forms a stable fluorescent dimer, $[pHPA]_2$. Monolayer cultures were washed with phenol red–free Hanks' buffered saline solution (HBSS) and incubated with 1.0 ml HBSS supplemented with glucose (6.5 mM), HEPES (1 mM), sodium bicarbonate (6 mM), pHPA (1.6 mM), and HRP (95 μg/ml) at 37°C for 1 h. The amount of H_2O_2 released into the buffer was measured spectrofluorometrically at 20 min intervals for 80 min using excitation and emission wavelengths of 323 and 400 nm, respectively. The fluorescent intensity of each sample was corrected for changes in pH. H_2O_2 absorbance at 240 nm was used as standard.

Statistical analysis

Statistical analysis was done using the one and two-way analysis of variance with Tukey's honestly significant difference test. Results from at least $n \geq 3$ with $p < 0.05$ were considered significant. All statistical analysis were done using SPSS computer software version 14.0 (SPSS Inc.).

Supplementary Material

Refer to Web version on PubMed Central for supplementary material.

REFERENCES

Bae YS, Kang SW, Seo MS, Baines IC, Tekle E, Chock PB, Rhee SG. Epidermal growth factor (EGF)-induced generation of hydrogen peroxide. Role in EGF receptor-mediated tyrosine phosphorylation. J Biol Chem 1997;272:217–221. [PubMed: 8995250]

Burdon RH, Gill V. Cellularly generated active oxygen species and HeLa cell proliferation. Free Radic Res Commun 1993;19:203–213. [PubMed: 8244089]

Fernandes AP, Holmgren A. Glutaredoxins: glutathione-dependent redox enzymes with functions far beyond a simple thioredoxin backup system. Antioxid Redox Signal 2004;6:63–74. [PubMed: 14713336]

Finkel T. Oxidant signals and oxidative stress. Curr Opin Cell Biol 2003;15:247–254. [PubMed: 12648682]

Goswami PC, Sheren J, Albee LD, Parsian A, Sim JE, Ridnour LA, Higashikubo R, Gius D, Hunt CR, Spitz DR. Cell cycle-coupled variation in topoisomerase IIalpha mRNA is regulated by the 3'-untranslated region. Possible role of redox-sensitive protein binding in mRNA accumulation. J Biol Chem 2000;275:38384–38392. [PubMed: 10986283]

Grana X, Reddy EP. Cell cycle control in mammalian cells: role of cyclins, cyclin dependent kinases (CDKs), growth suppressor genes and cyclin-dependent kinase inhibitors (CKIs). Oncogene 1995;11:211–219. [PubMed: 7624138]

Harman D. Aging: a theory based on free radical and radiation chemistry. J Gerontol 1956;11:298–300. [PubMed: 13332224]

Irani K, Xia Y, Zweier JL, Sollott SJ, Der CJ, Fearon ER, Sundaresan M, Finkel T, Goldschmidt-Clermont PJ. Mitogenic signaling mediated by oxidants in Ras-transformed fibroblasts. Science 1997;275:1649–1652. [PubMed: 9054359]

Kalen AL, Sarsour EH, Venkataraman S, Goswami PC. Mn-superoxide dismutase overexpression enhances G2 accumulation and radioresistance in human oral squamous carcinoma cells. Antioxid Redox Signal 2006;8:1273–1281. [PubMed: 16910775]

Kawamura N. Cytochemical and quantitative study of protein-bound sulfhydryl and disulfide groups in eggs of Arbacia during the first cleavage. Exp. Cell Res 1960;20:127–138. [PubMed: 14404965]

Kops GJ, Dansen TB, Polderman PE, Saarloos I, Wirtz KW, Coffer PJ, Huang TT, Bos JL, Medema RH, Burgering BM. Forkhead transcription factor FOXO3a protects quiescent cells from oxidative stress. Nature 2002a;419:316–321. [PubMed: 12239572]

Kops GJ, Medema RH, Glassford J, Essers MA, Dijkers PF, Coffer PJ, Lam EW, Burgering BM. Control of cell cycle exit and entry by protein kinase B-regulated forkhead transcription factors. Mol. Cell. Biol 2002b;22:2025–2036. [PubMed: 11884591]

Mauro F, Grasso A, Tolmach LJ. Variations in sulfhydryl, disulfide, and protein content during synchronous and asynchronous growth of HeLa cells. Biophys J 1969;9:1377–1397. [PubMed: 5353143]

McCord JM, Fridovich I. Superoxide dismutase. An enzymic function for erythrocuprein (hemocuprein). J Biol Chem 1969;244:6049–6055. [PubMed: 5389100]

Menon SG, Coleman MC, Walsh SA, Spitz DR, Goswami PC. Differential susceptibility of nonmalignant human breast epithelial cells and breast cancer cells to thiol antioxidant-induced G(1)-delay. Antioxid Redox Signal 2005;7:711–718. [PubMed: 15890017]

Menon SG, Goswami PC. A redox cycle within the cell cycle: ring in the old with the new. Oncogene 2007;26:1101–1109. [PubMed: 16924237]

Menon SG, Sarsour EH, Kalen AL, Venkataraman S, Hitchler MJ, Domann FE, Oberley LW, Goswami PC. Superoxide signaling mediates N-acetyl-L-cysteine-induced G1 arrest: regulatory role of cyclin D1 and manganese superoxide dismutase. Cancer Res 2007;67:6392–6399. [PubMed: 17616699]

Menon SG, Sarsour EH, Spitz DR, Higashikubo R, Sturm M, Zhang H, Goswami PC. Redox regulation of the G1 to S phase transition in the mouse embryo fibroblast cell cycle. Cancer Res 2003;63:2109–2117. [PubMed: 12727827]

Nevins JR. E2F: a link between the Rb tumor suppressor protein and viral oncoproteins. Science 1992;258:424–429. [PubMed: 1411535]

Oberley, LW. Superoxide dismutase. Boca Raton, Fla.: CRC Press; 1982.

Panus PC, Radi R, Chumley PH, Lillard RH, Freeman BA. Detection of H2O2 release from vascular endothelial cells. Free Radic. Biol. Med 1993;14:217–223. [PubMed: 8425723]

Rapkine L. Su Les Processus chimiques au cours de la division cellulaire. Ann. Physio. Physiochem. Biol 1931;7:382–418.

Rhee SG, Chang TS, Bae YS, Lee SR, Kang SW. Cellular regulation by hydrogen peroxide. J Am Soc Nephrol 2003;14:S211–S215. [PubMed: 12874433]

Sarsour EH, Agarwal M, Pandita TK, Oberley LW, Goswami PC. Manganese superoxide dismutase protects the proliferative capacity of confluent normal human fibroblasts. J Biol Chem 2005;280:18033–18041. [PubMed: 15743756]

Sherr CJ. Mammalian G1 cyclins. Cell 1993;73:1059–1065. [PubMed: 8513492]

Sundaresan M, Yu ZX, Ferrans VJ, Irani K, Finkel T. Requirement for generation of H2O2 for platelet-derived growth factor signal transduction. Science 1995;270:296–299. [PubMed: 7569979]

Tonks NK. Redox redux: revisiting PTPs and the control of cell signaling. Cell 2005;121:667–670. [PubMed: 15935753]

Tothova Z, Kollipara R, Huntly BJ, Lee BH, Castrillon DH, Cullen DE, McDowell EP, Lazo-Kallanian S, Williams IR, Sears C, Armstrong SA, Passegue E, DePinho RA, Gilliland DG. FoxOs are critical mediators of hematopoietic stem cell resistance to physiologic oxidative stress. Cell 2007;128:325–339. [PubMed: 17254970]

Tu BP, Kudlicki A, Rowicka M, McKnight SL. Logic of the yeast metabolic cycle: temporal compartmentalization of cellular processes. Science 2005;310:1152–1158. [PubMed: 16254148]

Zhang Y, Smith BJ, Oberley LW. Enzymatic activity is necessary for the tumor-suppressive effects of MnSOD. Antioxid Redox Signal 2006;8:1283–1293. [PubMed: 16910776]

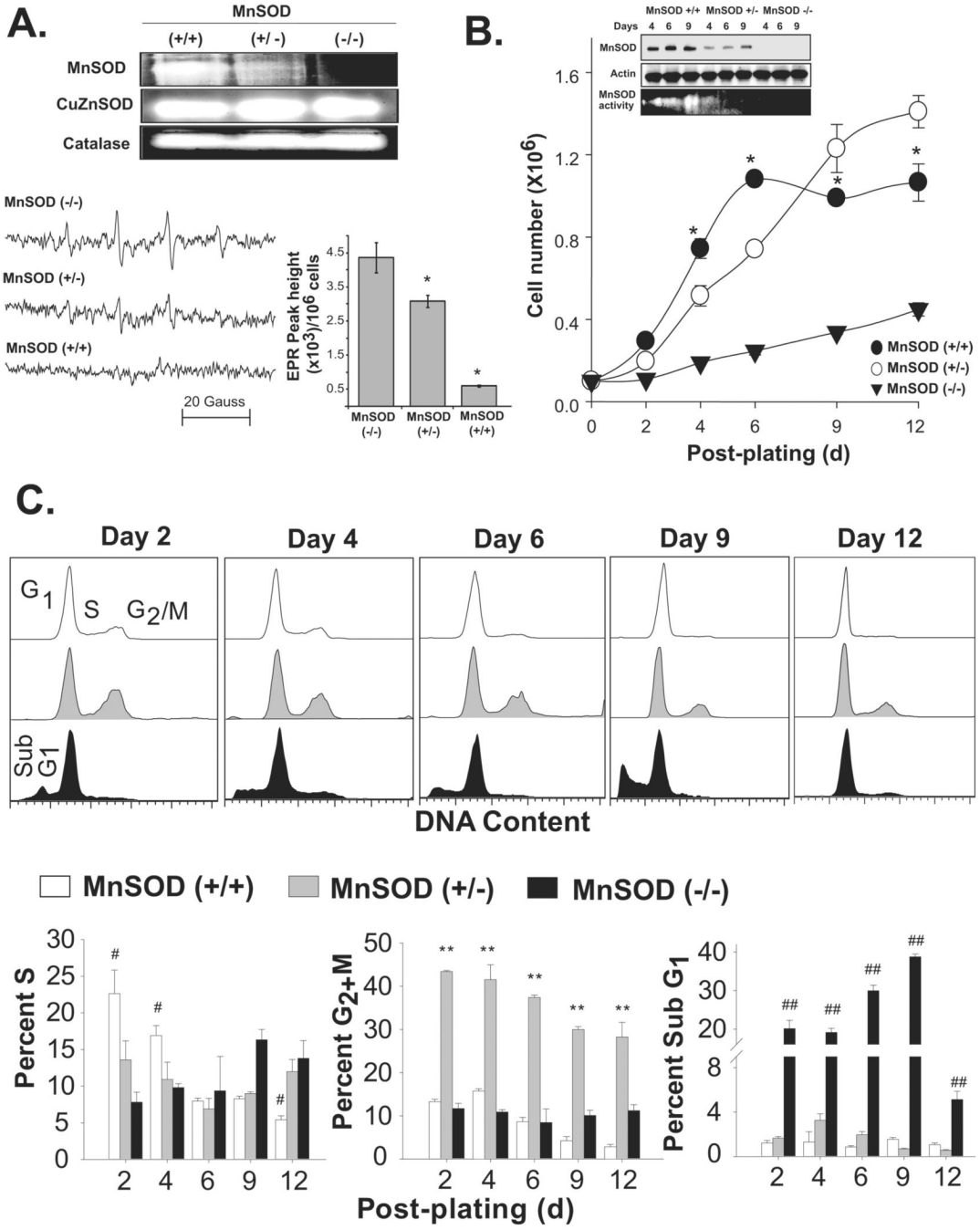

Figure 1. MnSOD activity regulates mouse embryonic fibroblasts' transitions between quiescent and proliferative growth

(A) Exponentially growing asynchronous cultures of MEFs were harvested and assayed for antioxidant enzyme activities by native gel-electrophoresis, and superoxide steady state levels by EPR spectroscopy. Representative EPR spectra are shown in lower left panel and EPR peak height calculated per million cells are shown in the right panel; asterisk indicates significant difference in MnSOD (+/−) and (+/+) compared to (−/−) MEFs, n=3, $p<0.05$. (B) Equal number of cells was plated in 60 mm dishes and cell number counted; inset: immunoblotting of MnSOD and actin, bottom panel shows MnSOD activity. Cells were fed with new media every 3d. Cell number represents total number of cells per 60 mm dish; asterisk indicates significant

difference in cell numbers in MnSOD (+/+) compared to (+/−) and (−/−) MEFs at indicated time points, n=3, $p<0.05$. (C) Representative DNA histograms of ethanol-fixed cells; percentages of S, G_2+M and cells with sub-G_1 DNA content were calculated using Cellquest software. (#) indicates significant difference in MnSOD (+/+) compared to (+/−) and (−/−) MEFs; (**) indicates significant difference in MnSOD (+/−) compared to (+/+) and (−/−) MEFs; (##) indicates significant difference in MnSOD (−/−) compared to (+/+) and (+/−) MEFs; n=3, $p < 0.05$.

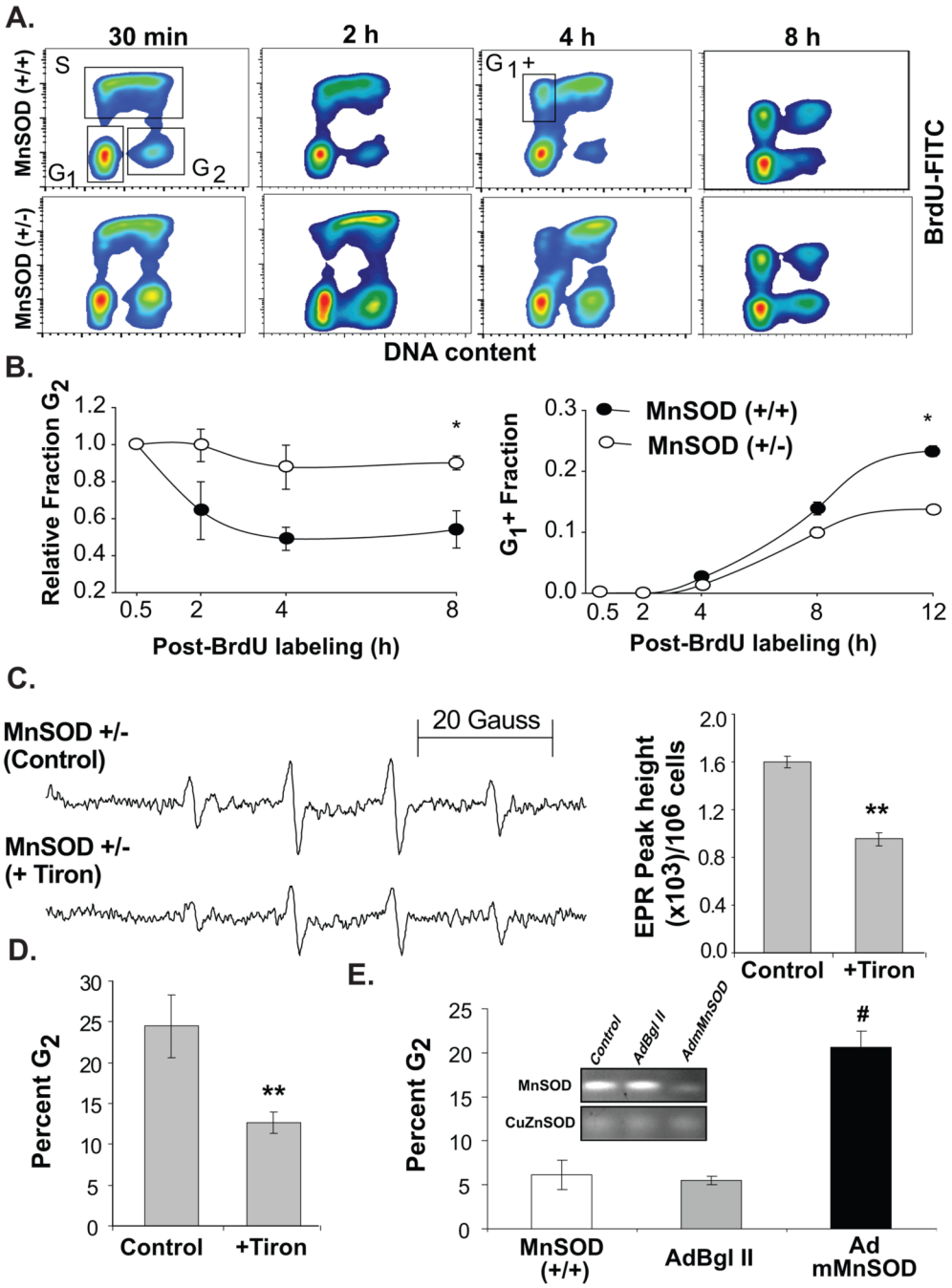

Figure 2. MnSOD activity and superoxide threshold levels are necessary for G_2 to M progression

(A) MEFs were pulse-labelled with BrdU and continued in culture in BrdU-free medium. Nuclei were isolated from ethanol-fixed cells and BrdU-positive S-phase and BrdU-negative G_1 and G_2 populations were assayed by flow cytometry; representative histograms are presented. (B) CellQuest software was used to calculate the relative fraction of G_2, and BrdU-positive cells that completed cell division (G_1 $^+$); asterisk indicates significant difference between the cell lines, n=3, $p<0.05$. (C) EPR spectroscopy measurements of superoxide steady state levels were performed in MnSOD (+/−) MEFs treated with 1 mM Tiron; PI-staining and flow cytometry measurement of DNA content was used to determine percent G_2 in cells harvested from replicate dishes (D). (**) indicates significant difference between Tiron treated

cells and controls; n=3, $p<0.05$. (E) In a separate experiment, exponentially growing asynchronous cultures of MnSOD (+/+) MEFs were mock-infected (first bar graph), infected with 50 MOI of adenoviruses carrying a control vector (AdBgl II) and dominant negative mutant MnSOD cDNA (AdmMnSOD; Zhang *et al.*, 2006). Cells were harvested at 48 h post-infection and fixed in ethanol. Ethanol-fixed cells were analyzed for DNA content by flow cytometry. The percentage of cells in G_2 calculated using CellQuest software; inset shows native gel-electrophoresis of MnSOD activity. (#) indicates significant difference in AdmMnSOD infected cells compared to control and AdBgl II infected MnSOD (+/+) MEFs, n=3, $p < 0.05$.

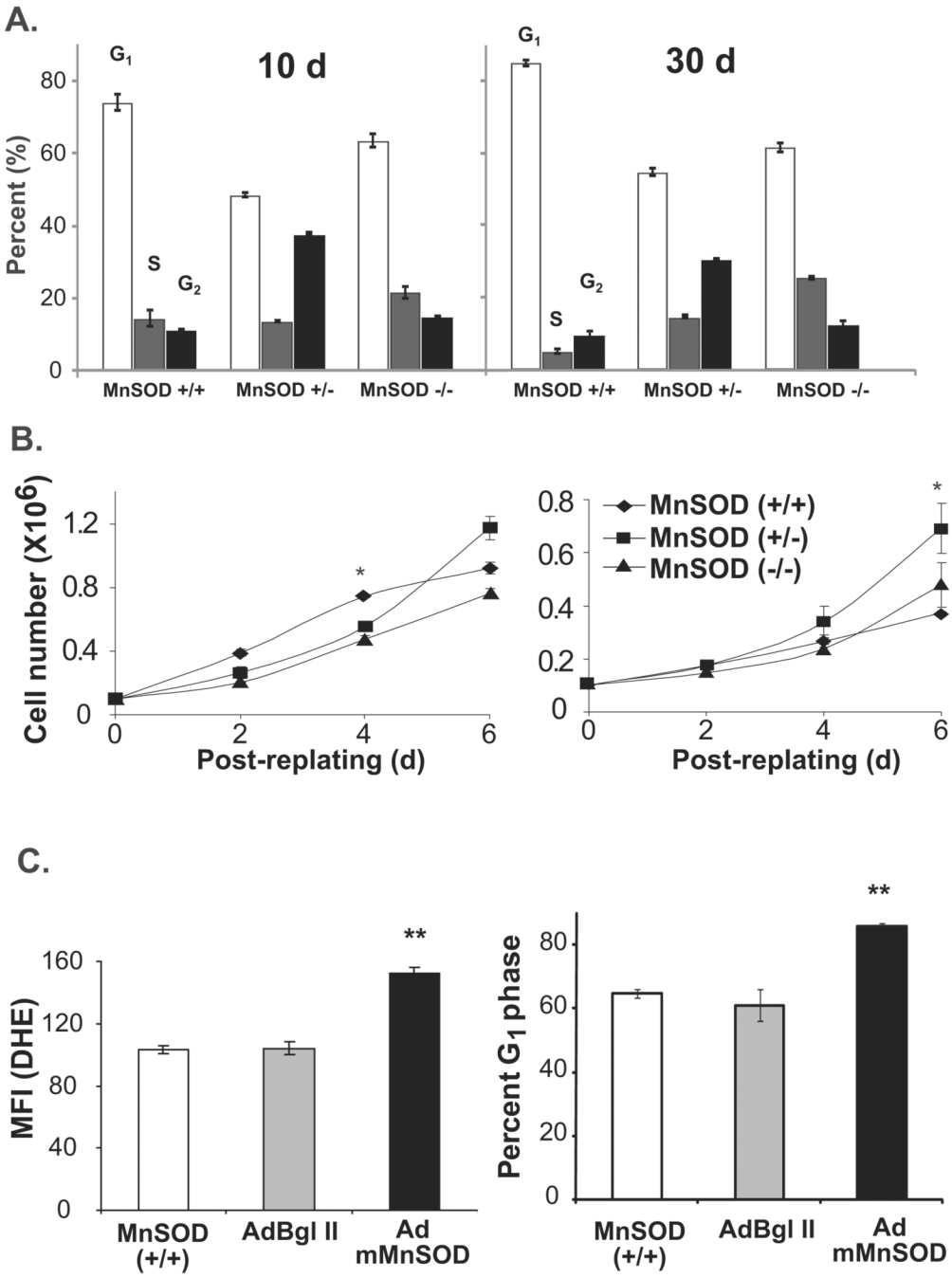

Figure 3. Appropriate levels of MnSOD activity are required for quiescent fibroblasts' entry into the proliferative cycle

(A) MEFs were cultured continuously for 10 and 30d of quiescent growth with change in media every 3d. Ethanol-fixed cells were stained with PI and cell cycle phase distributions analyzed by flow cytometry. (B) Cells from replicate dishes were re-plated at lower density and cell numbers counted at 2, 4, and 6d post-replating. Asterisk indicates significant difference between cell lines at the indicated time points, n=3, $p<0.05$. (C) Quiescent MnSOD (+/+) MEFs were mock-infected, infected with 50 MOI of AdBgl II and a dominant negative mutant form of MnSOD (AdmMnSOD) (Zhang *et al.* 2006). Quiescent control and infected cells were harvested for flow cytometry measurements of DHE-fluorescence. Cells from replicate dishes

were trypsinized and re-plated at a lower density. Re-plated cells were continued in culture for 48 h and harvested for flow cytometry measurements of DNA content. The percentage of G_1 calculated using CellQuest software. (**) indicates significant difference in AdmMnSOD infected cells compared to control and AdBgl II infected MnSOD (+/+) MEFs, n=3, $p < 0.05$.

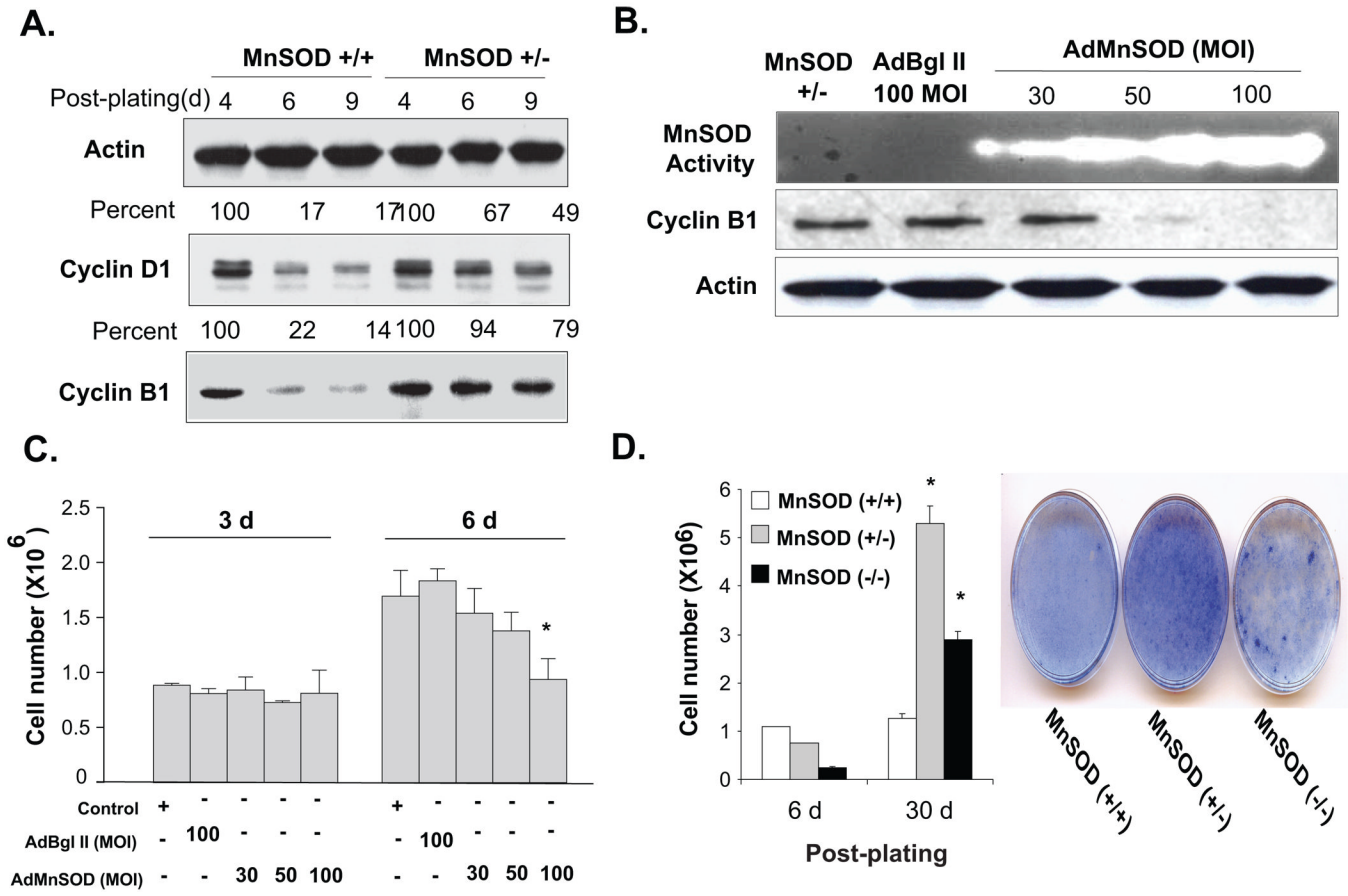

Figure 4. MnSOD activity and mitochondria-derived ROS levels are associated with changes in cyclin D1 and cyclin B1 protein levels during transitions between proliferative and quiescent growth

(A) Immunoblotting of cyclin D1, cyclin B1, and actin in MnSOD (+/+) and (+/−) fibroblasts at different days post-plating. (B) MnSOD (+/−) fibroblasts were infected with adenovirus carrying mouse MnSOD cDNA and analyzed for MnSOD activity and cyclin B1 protein levels. (C) Adenovirus infected MnSOD (+/−) fibroblasts harvested from replicate dishes were used to measure cell numbers at 3 and 6d post-infection. Asterisk indicates significant difference in MnSOD (+/−) cells over-expressing MnSOD compared to control and vector control at the indicated MOI, n=3, $p < 0.05$. (D) Fibroblasts growth at 6 and 30d cultures (left panel); coomassie stained 30d cultures (right panel). Asterisk indicates significant difference in MnSOD (+/−) and (−/−) compared to (+/+) MEFs, n=3, $p<0.05$.

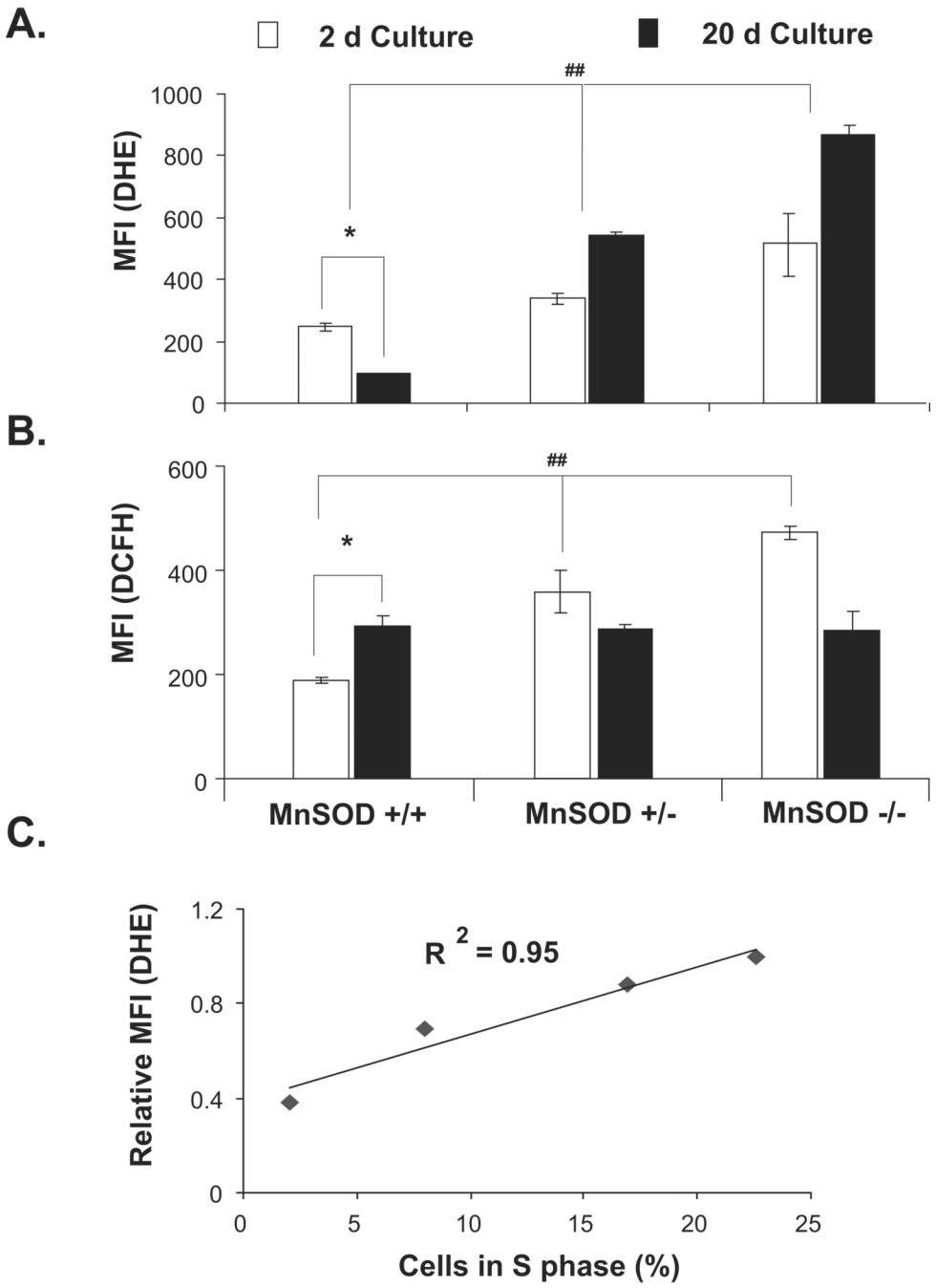

Figure 5. MnSOD activity regulates an "ROS switch" favouring a superoxide-signal regulating proliferation and a hydrogen peroxide-signal supporting quiescent growth

Fibroblasts representative of 2 and 20d cultures were incubated with (A) DHE (indicative of cellular superoxide levels) and (B) DCFH (indicative of cellular peroxide levels), and fluorescence measured by flow cytometry. MnSOD (+/+) 2d fibroblasts represent exponential cultures (~25% S-phase) while 20d cultures represent quiescent growth (~2 % S-phase). (C) Regression plot for the correlation between superoxide levels and percent S. MnSOD (+/+) MEFs were harvested at different days post-plating and analyzed for DHE-fluorescence and percent S-phase by flow cytometry. Asterisk indicates significant difference between 2 and

20d MnSOD (+/+) MEFs; (##) indicates significant difference between MnSOD (+/+) compared to (+/−) and (−/−) MEFs. n=3, $p < 0.05$.

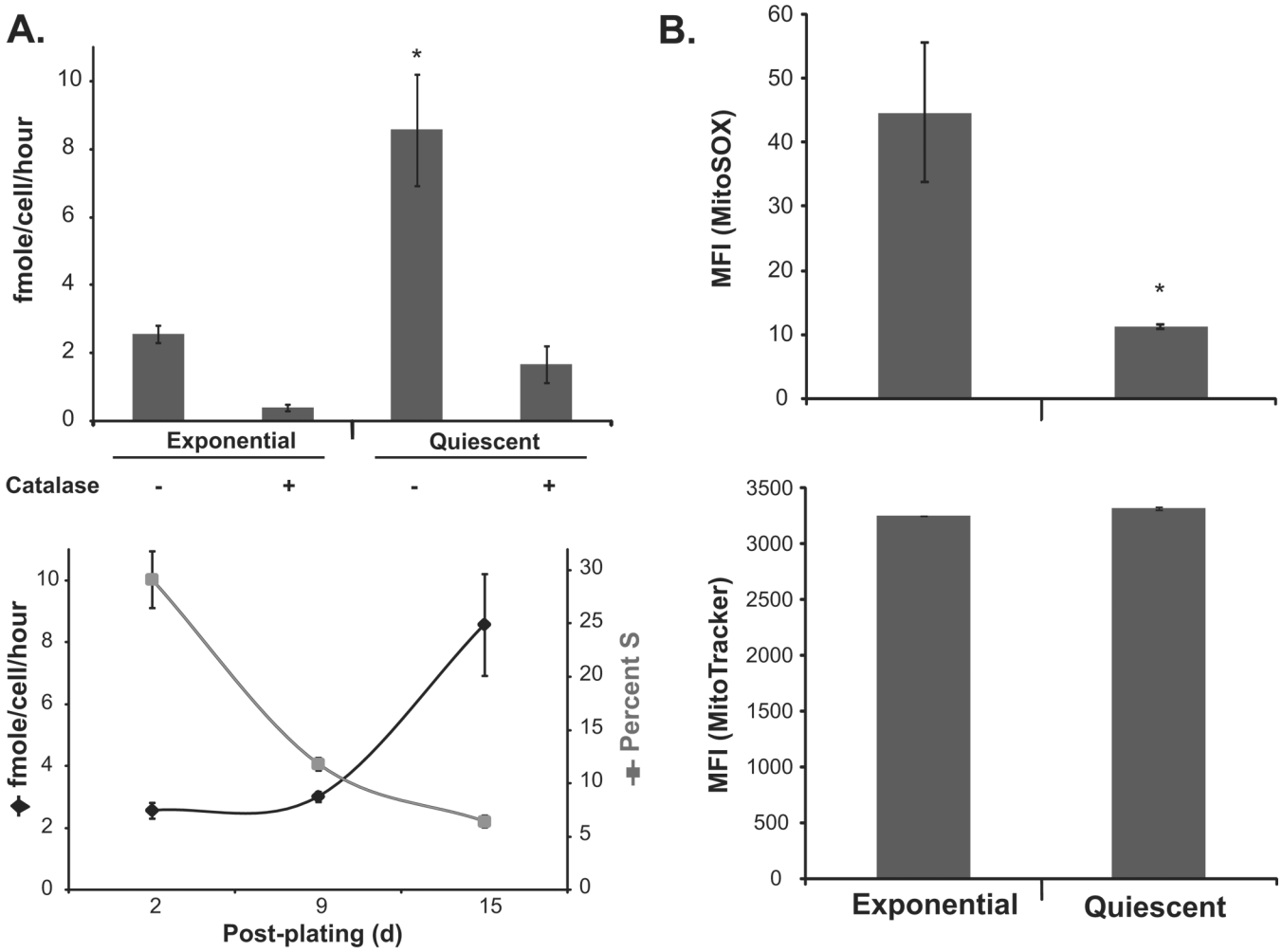

Figure 6. Mitochondria derived ROS regulate transitions between quiescent and proliferative growth

(A) HRP-pHPA assay of extracellular hydrogen peroxide released from exponential and quiescent MnSOD (+/+) MEFs. The specificity of the assay for measurement of hydrogen peroxide was determined by adding catalase in the reaction buffer. Asterisk indicates significant difference in quiescent MnSOD (+/+) MEFs compared to exponential cultures, n=3, $p<0.05$. The percent S-phase and amount of extracellular hydrogen peroxide levels are shown in the bottom panel. (B) Exponential and quiescent MnSOD (+/+) MEFs were stained with MitoSox (upper panel) and MitoTracker (bottom panel), and fluorescence analyzed by flow cytometry. Asterisk indicates significant difference in quiescent compared to exponential cultures, n=3, $p<0.05$.

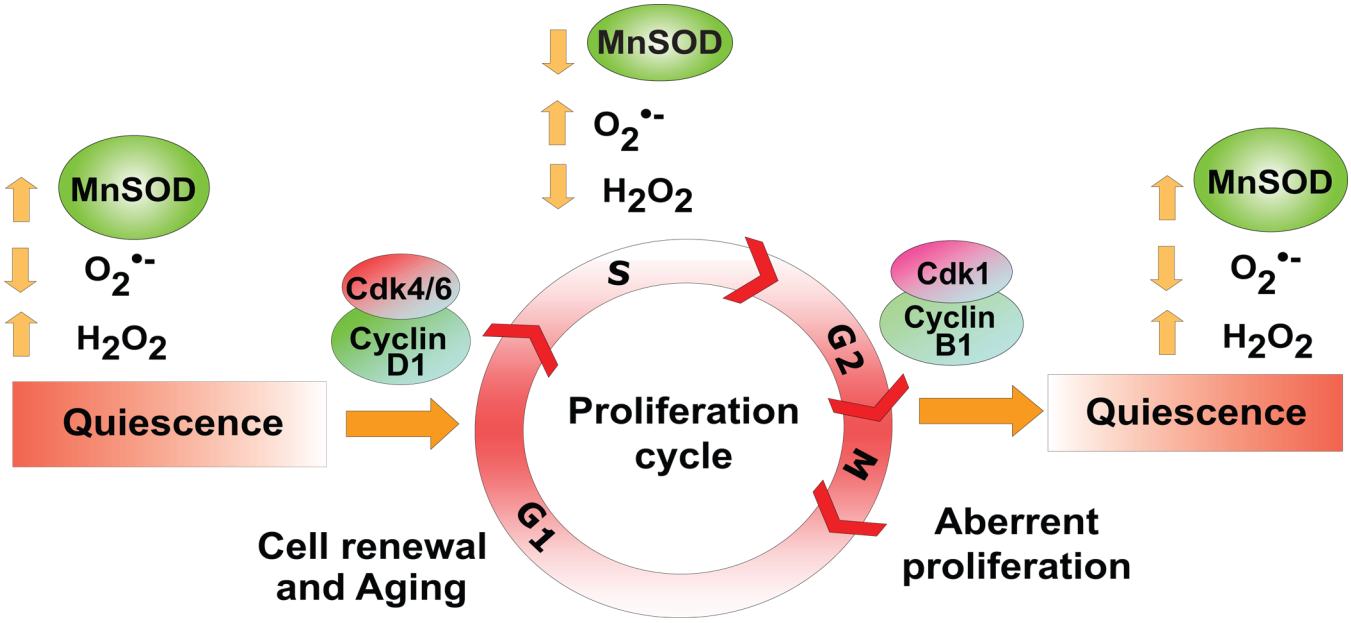

Figure 7. MnSOD activity and mitochondria derived ROS-levels regulate transitions between quiescence and proliferative growth

A schematic illustration of MnSOD activity regulating entry into and exit from the proliferative cycle. A loss in the redox-control of this regulation could have myriad of cellular effects including aberrant proliferation, defects in cell-renewal, cancer and cellular aging.